

Phase properties of a zigzag chain lattice gas with Coulomb interactions

T. C. King and Y. K. Kuo*

Synchrotron Radiation Research Center, Hsinchu Science-Based Industrial Park, Hsinchu, 300 Taiwan, Republic of China
and Department of Physics, National Dong-Hwa University, 974 Taiwan, Republic of China

(Received 12 March 2003; published 19 September 2003)

It has been reported that the phase transitions found in the quasi-one-dimensional sulfide $\text{KCu}_{7-x}\text{S}_4$ are most likely due to vacancy ordering involving Cu^+ -ion diffusion along the $\text{Cu}(2)$ - $\text{Cu}(2)$ zigzag chains. Our previous studies with both a self-consistent method and Monte Carlo simulations confirmed that phase transitions indeed exist in a one-dimensional (1D) lattice gas system in which vacancy ordering is involved. In this paper, we calculate the more nearly real case of $\text{KCu}_{6.88}\text{S}_4$ and further investigate the angular dependence of the phase properties in a partially occupied 1D zigzag chain with various particle occupancies. The calculated results suggest that the phase transitions that occur in the quasi-one-dimensional material $\text{KCu}_{7-x}\text{S}_4$ are presumably due to both intrachain and interchain interactions between the partially occupied Cu^+ zigzag chains. Most interestingly, we found that the average particle distribution of the lowest free energy state is a linear superposition of two other solutions with different particle distributions for occupancy $n_{av} = 1/2$.

DOI: 10.1103/PhysRevE.68.036116

PACS number(s): 64.60.Cn, 05.10.-a, 45.50.Jf

I. INTRODUCTION

Previously, we proposed a long range mean-field (LRMF) method to simplify the Hamiltonian of a one-dimensional (1D) straight chain with $1/r$ Coulomb repulsive interactions. This is relevant to the study of vacancy ordering transitions in quasi-one-dimensional (Q1D) materials such as $\text{KCu}_{7-x}\text{S}_4$. We self-consistently calculated all possible solutions of average particle number distributions in such a system [1]. The numerical results show that phase transitions do indeed exist in a 1D lattice gas system in which vacancy ordering is involved and the system exhibits complex thermodynamic properties. The properties of the phase transitions are extremely sensitive to the occupancy n_{av} (number of particles/number of lattice sites), and each simple rational occupancy n_{av} has a unique phase diagram. More recently, we used Monte Carlo simulations to extend our self-inconsistence method by introducing the effect of thermal fluctuations on the phase transitions in a 1D ordering system [2]. In this study, we find hysteretic behavior near the phase transition at low temperature with $n_{av} = 3/4$. This agrees well with our experimental findings in the quasi-one-dimensional sulfide $\text{KCu}_{7-x}\text{S}_4$ system [3] and supports the possible scenario of vacancy ordering in the 1D Cu^+ chain.

Our previous work focused on a 1D lattice gas system on a partially occupied straight chain. However, structurally $\text{KCu}_{7-x}\text{S}_4$ forms $\text{Cu}(2)$ - $\text{Cu}(2)$ zigzag chains along the c axis [4,5]. For instance, the zigzag angle (denoted by θ) is 115.388° for $\text{KCu}_{6.66}\text{S}_4$ and 112.74° for $\text{KCu}_{6.88}\text{S}_4$ ($\theta = 180^\circ$ for a straight chain) [4,5]. It was proposed that the phase transitions that occur in $\text{KCu}_{7-x}\text{S}_4$ are caused by an ordering of the vacancies in these $\text{Cu}(2)$ - $\text{Cu}(2)$ zigzag chains [3]. Therefore, it may be crucial to study the angular dependence of the 1D lattice gas system to understand the properties of phase transitions in the $\text{KCu}_{7-x}\text{S}_4$ system.

In this paper, we perform a real-case calculation on $\text{KCu}_{6.88}\text{S}_4$ ($n_{av} = 0.72$) with $\theta = 112.74^\circ$. We also study the properties of phase transitions in partially occupied 1D zigzag chains (PODZ) with various angles θ and occupancy n_{av} . As the phase properties of the PODZ with Coulomb repulsive interactions are extremely complex, we only present the two simplest occupancy cases, i.e., $n_{av} = \frac{1}{2}$ and $\frac{2}{3}$ in this paper. Our calculated results suggest that the phase transitions that occur in the quasi-one-dimensional material $\text{KCu}_{7-x}\text{S}_4$ are presumably due to both intrachain and interchain interactions between the partially occupied Cu^+ zigzag chains. That is, these phase transitions exhibited in $\text{KCu}_{7-x}\text{S}_4$ are mainly a three-dimensional phenomenon, in agreement with the x-ray diffraction and TEM results [4,5]. We also found that the average particle distribution of the lowest free energy state is a linear superposition of two other solutions with different particle distribution for occupancy, $n_{av} = 1/2$. In Sec. II the long range mean-field method and our formulation are briefly described. In Sec. III we show our calculated results on $n_{av} = 0.72$ with $\theta = 112.74^\circ$, $n_{av} = \frac{1}{2}$ and $\frac{2}{3}$ as well as their corresponding angular dependence. The discussion and summary are presented in Sec. IV.

II. LONG RANGE MEAN-FIELD METHOD

The Hamiltonian of a 1D zigzag chain with $1/r$ Coulomb repulsive interactions can be obtained by modifying the straight chain Hamiltonian in Ref. [1]:

$$\mathbf{H} = \sum_{i=1}^{N_s} \sum_{j>i} \frac{J}{r_{ij}/a} n_i n_j, \quad (1)$$

where J is the Coulomb potential energy between two nearest neighbor particles, n_i ($n_i = 0$ or 1) is the particle number of site i , r_{ij} is the distance between the site i and j , a is the distance between the nearest neighbor sites, which is held constant in our calculations, and N_s is the number of total sites in the 1D zigzag chain. Here we assume that there are N_i ions evenly distributed over N_s lattice sites ($N_i < N_s$ for a

*Electronic address: ykkuo@mail.ndhu.edu.tw

partially occupied chain), and use open boundary conditions to avoid the divergence of the Hamiltonian. We simplify Eq. (1) into a LRMF system by assuming that the 1D zigzag chain can be divided into many identical segments, each of which contains N_o ions distributed over N_w sites (so that the average occupancy $n_{av} = N_o/N_w = N_i/N_s$, as ions are uniformly distributed). Under this assumption, the thermodynamic averages of the particle distributions of each segment are identical. We exactly consider the interactions between particles within the segment at the *center* of the 1D lattice gas and replace the interactions of all other particles by a local field which is the thermodynamic average of the interactions acting on the considered segment by all particles outside this segment. We thus obtain a LRMF Hamiltonian described by

$$\mathbf{H}_{MF} = J \sum_{(i,j)} \frac{n_i n_j}{r_{ij}/a} + \sum_{i=1}^{N_w} n_i h_i, \quad (2)$$

where $\sum_{(i,j)}$ sums over all pairs of particles in the considered segment, n_i ($n_i = 0$ or 1 and $i = 1$ to N_w) is the particle

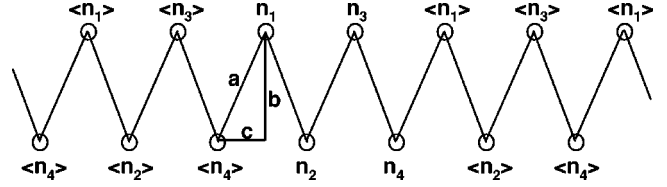


FIG. 1. An illustration of a one-dimensional zigzag chain simplified by LRMF with $N_w = 4$. The particle number of the sites outside the considered segment is replaced by the thermal average of the corresponding sites in the considered segment.

number of the i th site, and the h_i is the local mean field acting on the site i which is a function of the zigzag angle θ . Figure 1 shows a zigzag chain simplified by the LRMF method with $N_w = 4$. The particle numbers of the sites outside the considered segment are replaced by the thermal average of the corresponding sites in the considered segment. In this simplified chain the local mean field acting on site 1 is the superposition of all the Coulomb potentials outside the considered segment, which can be written as

$$h_1 = \frac{\langle n_4 \rangle}{\sqrt{b^2 + c^2}} + \frac{\langle n_3 \rangle}{2c} + \frac{\langle n_2 \rangle}{\sqrt{b^2 + (3c)^2}} + \frac{\langle n_1 \rangle}{4c} + \frac{\langle n_4 \rangle}{\sqrt{b^2 + (5c)^2}} + \frac{\langle n_3 \rangle}{6c} + \frac{\langle n_2 \rangle}{\sqrt{b^2 + (7c)^2}} + \frac{\langle n_1 \rangle}{8c} + \dots + \frac{\langle n_1 \rangle}{4c} + \frac{\langle n_2 \rangle}{\sqrt{b^2 + (5c)^2}} + \frac{\langle n_3 \rangle}{6c} + \frac{\langle n_4 \rangle}{\sqrt{b^2 + (7c)^2}} + \frac{\langle n_1 \rangle}{8c} + \frac{\langle n_2 \rangle}{\sqrt{b^2 + (9c)^2}} + \frac{\langle n_3 \rangle}{10c} + \frac{\langle n_4 \rangle}{\sqrt{b^2 + (11c)^2}} + \dots, \quad (3)$$

where $b = a \cos \theta/2$ and $c = a \sin \theta/2$. We can rewrite the above equation in a simplified form:

$$h_1 = S_{11} \langle n_1 \rangle + S_{12} \langle n_2 \rangle + S_{13} \langle n_3 \rangle + S_{14} \langle n_4 \rangle, \quad (4)$$

where the S_{ij} are the structure relationships between site i and $\langle n_j \rangle$, which are functions of θ . Then the LRMF Hamiltonian is expressed as

$$\mathbf{H}_{MF} = J \sum_{(i,j)} \frac{n_i n_j}{r_{ij}/a} + \sum_{i=1}^{N_w} n_i \sum_{j=1}^{N_w} S_{ij} \langle n_j \rangle. \quad (5)$$

The free energy of Eq. (2) is

$$F_{MF} = -kT \ln \text{Tr}[\exp(-\mathbf{H}_{MF}/kT)], \quad (6)$$

where k is the Boltzmann constant. The thermodynamic average particle number at the site i is then described by

$$\langle n_i \rangle = \frac{\text{Tr}[n_i \exp(-\mathbf{H}_{MF}/kT)]}{\text{Tr}[\exp(-\mathbf{H}_{MF}/kT)]}. \quad (7)$$

As N_s , N_w , N_o , and the temperature T are given, we can numerically calculate the self-consistent solutions of $\{\langle n_i \rangle\}$ in each segment with Eq. (7). Here $\{\langle n_i \rangle\}$ has N_w elements and $\sum \langle n_i \rangle = N_o$. Since the x-ray diffraction patterns are determined by the average particle number distributions, intu-

itively each element in $\{\langle n_i \rangle\}$ is a member of a reasonable set of order parameters. In our calculations we assume $N_s = 600\,000$ and $N_w = 12$. It is noted that the calculated properties of PODZ's with various N_w and N_s are essentially the same, except for small quantitative differences. For convenience, we further define an order index q by

$$q = \frac{\sum_{i=1}^{N_w} (\langle n_i \rangle - n_{av})^2}{N_o(1 - n_{av})^2 + (N_w - N_o)n_{av}^2}, \quad (8)$$

where $0 \leq q \leq 1$. When $q = 0$, all the $\langle n_i \rangle$ are equal to n_{av} , which corresponds to the state at very high temperature. When $q = 1$, the system is completely ordered, $\langle n_i \rangle$ is equal to either 0 or 1, corresponding to the state at absolute zero. Note that here we neglect the effect of anions in our calculations. In the real crystal structure of $\text{KCu}_{7-x}\text{S}_4$ contains vacancies only on the positive Cu ion sites, the negative S ions are held in their lattice sites [4,5]. The contribution of anions to the system is to build up a steady electrical potential, which is macroscopically even and microscopically periodic. Therefore, to simplify our model, we use the approximation similar to that of jellium model in which the negative ions distribute uniformly in space and can be neglected [6].

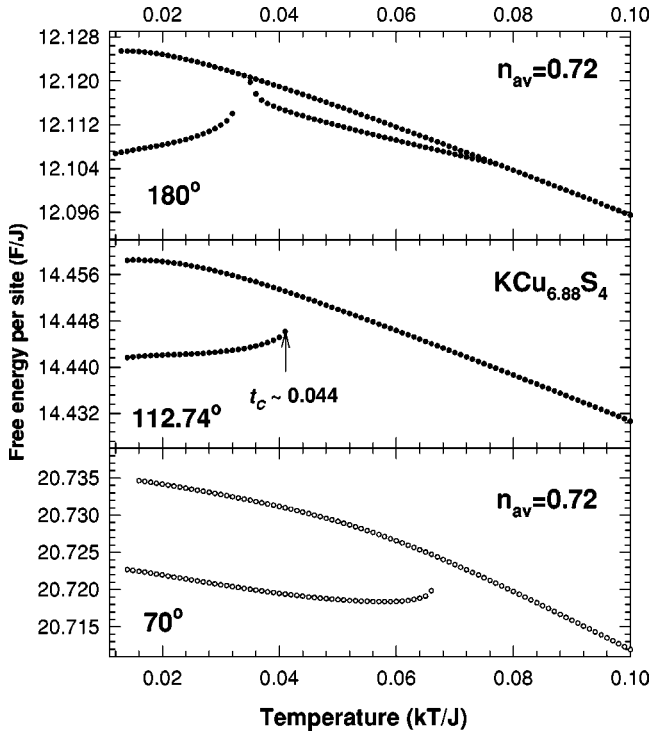


FIG. 2. A real-case calculation of $\text{KCu}_{6.88}\text{S}_4$ with $n_{av}=0.72$ ($=18/25$) for $\theta=180^\circ$, 112.74° , and 70° .

Thus we only consider the interactions between positive ions that could move around the lattice sites and order.

III. RESULTS

A. $n_{av}=0.72$

In this section we first present a real-case calculation of $\text{KCu}_{6.88}\text{S}_4$ with $n_{av}=0.72$ ($=18/25$) and compare with experimental findings. In the real crystal structure of $\text{KCu}_{6.88}\text{S}_4$, the angle for the partially occupied Cu^+ zigzag chain is 112.74° . In Fig. 2, we show the evolution of the calculated results of free energy F versus temperature t for $\theta=180^\circ$, 112.74° , and 70° . As shown in Fig. 2(a), there are three phase transitions (two second-order transitions, in which the free energies, their derivatives, and the order parameters smoothly approach each other; and one first-order transition, in which the first derivatives of the free energies and the order parameters are not the same at the transition) that exist in the $n_{av}=0.72$ system when $\theta=180^\circ$. Note that 180° corresponds to a straight chain. As the angle decreases, the system becomes simpler and exhibits only one first-order phase transition. For $\theta=112.74^\circ$, t_c is about 0.044 and increases to about 0.067 for $\theta=70^\circ$. By taking the $\text{Cu}(2)\text{-Cu}(2)$ bond distance to be approximately 3 Å, the Coulomb potential energy between two nearest neighbor particles J can be estimated to be 4.8 eV. Here we ignore the fact that the Coulomb interaction would be shielded in the conducting crystals. Thus the calculated transition temperature $T_C = 0.044J/k$ in the $n_{av}=0.72$ zigzag chain ($\theta=112.74^\circ$) is approximately 2400 K. Experimentally, there are two phase transitions observed in $\text{KCu}_{6.88}\text{S}_4$ at about 200 K. The dis-

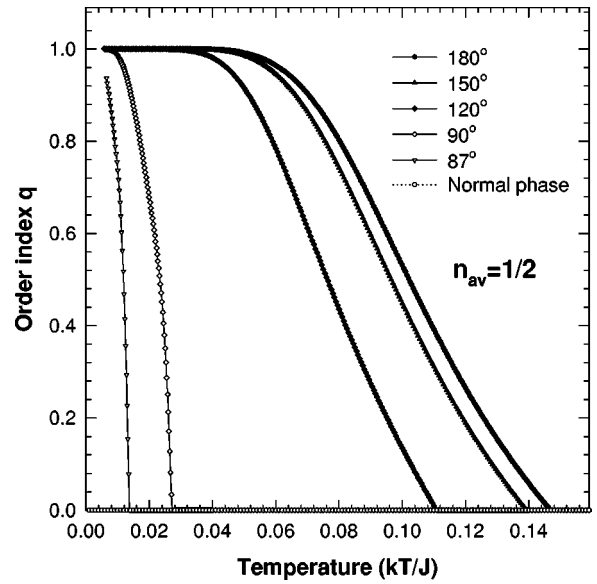


FIG. 3. The order indices q vs temperature t for $\theta>87^\circ$ with $n_{av}=0.5$ zigzag chain. The second-order phase transition temperature t_c decreases as θ decreases.

crepancy between our calculations and experimental results may be due to the following reasons.

(1) The interchain interactions between the zigzag chains, not considered in our model, should play important roles in the phase properties of $\text{KCu}_{7-x}\text{S}_4$. The calculation of exact effect on interchain interactions to the phase properties of 1D lattice gas system is now being carried out.

(2) The shielding effect of the Coulomb interaction between neighboring particles should be taken into account in the model to obtain consistent transition temperatures between theory and experiment.

(3) The mean-field approximation we employed in this model. According to our previous calculations, as the number of sites in a segment increases (closer to the exact result) the transition temperature shifts toward lower temperature (see Figs. 1 and 2 of Ref. [1]).

B. $n_{av}=1/2$

According to our previous studies [1,2], a second-order vacancy ordering transition occurs at about $t=0.15$ in the straight chain lattice gas system with $n_{av}=1/2$. For $t > 0.15$, the $\{\langle n_i \rangle\}$ has a single numerical solution with all the $\langle n_i \rangle$'s being 0.5, herein called the normal phase. This state corresponds to the completely disordered state. For $t < 0.15$, another solution with lower free energy state having average particle numbers repeating themselves every two sites, i.e., $\{\langle n_i \rangle\} = \{n_1, n_2\}$ appears, herein called the special phase. In Fig. 3, we show the results for the order index as a function of temperature t for angles θ from 180° to 87° . It can be seen that the transition temperature decreases as the angle decreases and the special phase disappears at angle $\theta = 85.8^\circ$. At this angle, the transition temperature between the normal state and the special state approaches zero.

Before the disappearance of the special phase, a new phase, herein called the mixed phase, with the lowest free

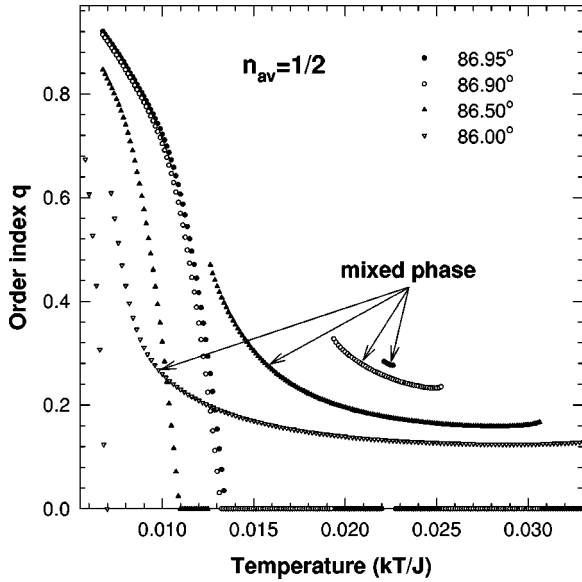


FIG. 4. The order indices q vs temperature t for $86^\circ < \theta < 86.95^\circ$ with $n_{av}=0.5$. A new phase called the “mixed phase” appears at $\theta \approx 86.96^\circ$ and disappears at $\theta \approx 86^\circ$.

energy emerges at angle $\theta = 86.95^\circ$. The period of the average particle distribution of the mixed phase is every four sites, i.e., $\{\langle n_i \rangle\} = \{n_1, n_2, n_3, n_4\}$. In Fig. 4, we show the details of order index as a function of temperature t for several angles θ between 86.95° and 86° , an intriguing evolution of a physical property that occurs within this one degree. It is clearly seen in this figure that the mixed state exists over a wider temperature range as the angle decreases. For $\theta < 85.8^\circ$, the special phase completely disappears. However, another special phase, herein called the dual special phase, with average distribution period every four sites, i.e., $\{\langle n_i \rangle\} = \{n_1, n_1, n_2, n_2\}$ appears. The transition between the normal state and the dual special phase is second order. Actually the dual special phase can be viewed as two neighboring straight chains, both in the special phase. In other words, for $\theta > 85.8^\circ$ the zigzag chain still shows the properties of a single straight chain, while for $\theta < 85.8^\circ$ the zigzag chain possesses the character of a double chain. In Fig. 5, we show the results of the order index as a function of temperature t for several angles θ between 85° and 15° . Both the mixed phase and the dual special phase exist between these angles. Notice that the transition temperature from the normal state to the dual special phase increases as the angle decreases, in contrast to the results shown in Fig. 3.

For $\theta > 50^\circ$ the mixed phase has the lowest free energy, while the dual special phase has the lowest free energy for $\theta < 47^\circ$. The order indices of the mixed phase and the dual special phase approach each other as the angle decreases, and eventually those two phases intersect and overlap around $\theta = 15^\circ$, as shown in Fig. 5. We found that the mixed phase is a linear combination of the special phase and the dual special phase. The average particle distribution $\{\langle n_i \rangle\}$ of the mixed phase can be exactly written as $\{n_1, n_2, n_1, n_2\}_M = a\{n_1, n_2, n_1, n_2\}_S + b\{n_1, n_1, n_2, n_2\}_D$, where $\{n_1, n_2, n_3, n_4\}_M$, $\{n_1, n_2, n_1, n_2\}_S$, and $\{n_1, n_1, n_2, n_2\}_D$ are

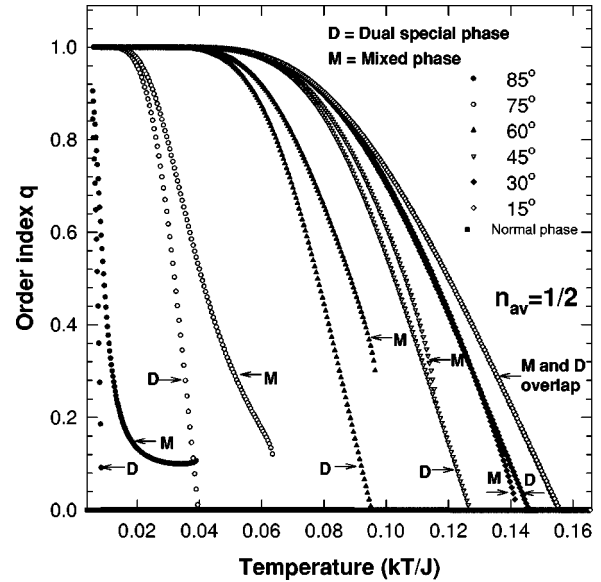


FIG. 5. The order indices q vs temperature t for $15^\circ < \theta < 85^\circ$ with $n_{av}=0.5$. Both the mixed phase and the dual special phase exist within these angles. The transition temperature between the normal state and the dual special phase increases as the angle decreases.

the average particle distributions for the mixed phase, the special phase, and the dual special phase, respectively. The a and b are the expansion coefficients with $a + b = 1$. In the upper panel of Fig. 6, we show the temperature dependence of the individual average particle distributions with the lowest free energy phase for $\theta = 86.5^\circ$. For $t > 0.03$ the system is in the normal phase, for $0.012 < t < 0.03$ the system is in the mixed phase, and for $0.01 < t$ the system is in the special

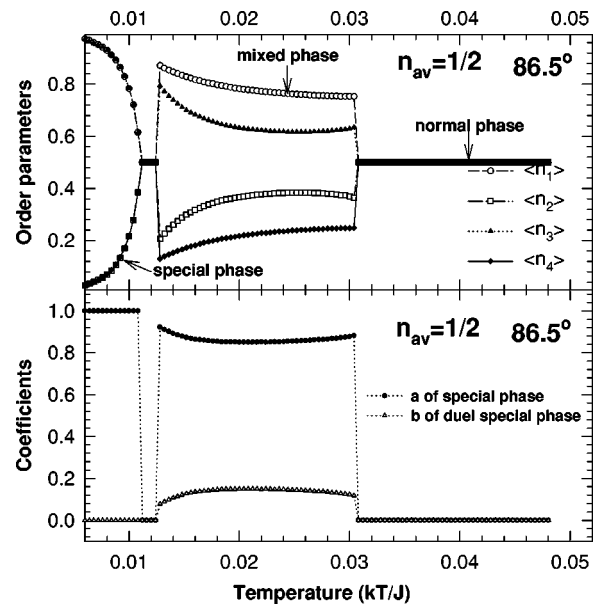


FIG. 6. Upper panel: temperature dependence of the individual average particle distributions with the lowest free energy phase for $\theta = 86.5^\circ$ with $n_{av}=0.5$. Lower panel: the coefficients a and b of the mixed phase for $\theta = 86.5^\circ$ with $n_{av}=0.5$.

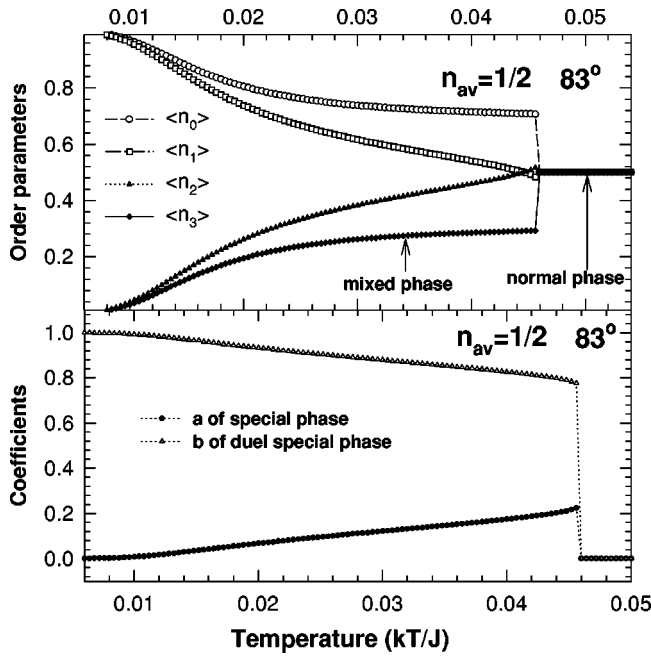


FIG. 7. Upper panel: temperature dependence of the individual average particle distributions with the lowest free energy phase for $\theta=83^\circ$ with $n_{av}=0.5$. Lower panel: the coefficients a and b of the mixed phase for $\theta=83^\circ$ with $n_{av}=0.5$. The mixed phase is mostly composed of the double chain mode at this angle.

phase. Clearly three phase transitions exist in this system, two first-order transitions with a discontinuous dF/dT occur at about $t=0.03$ and 0.012 , and one second-order (continuous) transition occurs at about $t=0.01$. The lower panel of Fig. 6 shows the coefficients a and b of the mixed phase versus temperature. For $0.012 < t < 0.03$ the mixed phase is composed of approximately 80% single chain mode (special phase) and 20% double chain mode (dual special phase). For $0.01 < t$ the system is 100% single chain mode (special phase).

In Fig. 7, we show the temperature dependence of the individual average particle distributions with the lowest free-energy phase for $\theta=83^\circ$. As demonstrated in Figs. 6 and 7, there is a considerable difference in the phase properties between $\theta=86.5^\circ$ and $\theta=83^\circ$. For $\theta=83^\circ$, the system is in the normal phase for $t > 0.046$ and in the mixed phase for $t < 0.046$. There is only one first-order transition, at about $t=0.046$ in this case. Besides, as shown in the lower panel of Fig. 7, the mixed phase is composed mostly of the double chain mode (dual special phase), i.e., a is much less than b . As t decreases, the coefficients a approach zero. The calculated ground state ($t=0$) particle distribution for $\theta=83^\circ$ is $\{1,1,0,0\}$, completely double chain mode with $a=0$. According to our calculations, the system would exhibit more of the double chain character as θ decreases. This result makes physical sense because the zigzag chain gradually turns into two well-separated straight chains as θ becomes smaller.

C. $n_{av}=2/3$

For $n_{av}=2/3$, the angular dependence of the phase properties in the partially occupied zigzag chain is much more

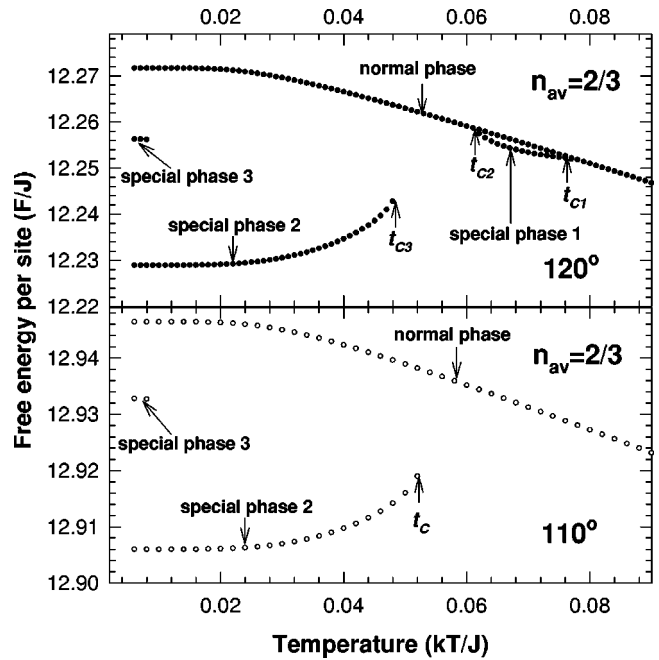


FIG. 8. The free energy F of the system as a function of temperature t for $\theta=120^\circ$ (upper panel) and $\theta=110^\circ$ (lower panel) with $n_{av}=2/3$.

complex than in the case of $n_{av}=1/2$. We found that there are seven possible phases in the $n_{av}=2/3$ zigzag chain, namely, the normal phase and special phases 1 to 6. All these seven phases have distinct average particle distributions $\{\langle n_i \rangle\}$ and exist in various angle intervals and temperature ranges. In Fig. 8, we show the free energy F of the system as a function of temperature t for $\theta=120^\circ$ (upper panel) and $\theta=110^\circ$ (lower panel). For $\theta=120^\circ$, the properties of the system are similar to those of the straight chain system, see Fig. 4 of Ref. [1]. At this angle, there are two second-order phase transitions in this system at about $t=0.08$ and $t=0.061$ and a first-order transition at about $t=0.048$. The phase existing at all temperatures is the normal phase with average particle distribution $\{n_1, n_2, n_3, n_3, n_2, n_1\}$. The phase existing between $0.061 < t < 0.08$ is special phase 1 with average particle distribution $\{n_1, n_2, n_3, n_4, n_5, n_6\}$. The phase existing below $t < 0.044$ is special phase 2, also with average particle distribution $\{n_1, n_2, n_3, n_4, n_5, n_6\}$, but with differing values of n_i . Special phase 3 exists only at very low temperatures ($t < 0.01$) and has average particle distribution $\{0.5, 1, 0.5, 0.5, 1, 0.5\}$. As the angle decreases, the temperature range of special phase 1 is diminished. As shown in the lower panel of Fig. 8, special phase 1 completely disappears at $\theta=110^\circ$ and therefore only one first-order transition exists at this angle. As the angle further decreases, the solution of special phase 3 will also gradually disappear, and the free energy of the normal phase becomes smaller in the low temperature range. For $\theta < 49^\circ$, the free energy of the normal phase is lower than that of the special phase 2 for $t < 0.05$. In Figs. 9(a)–9(d), we show the evolution of $F-t$ plots from $\theta=45^\circ$ to $\theta=33^\circ$. At $\theta=45^\circ$, the existing stable phases are the normal phase, special phase 2 and special phase 3. The normal phase develops a peak at about $t=0.09$. For t

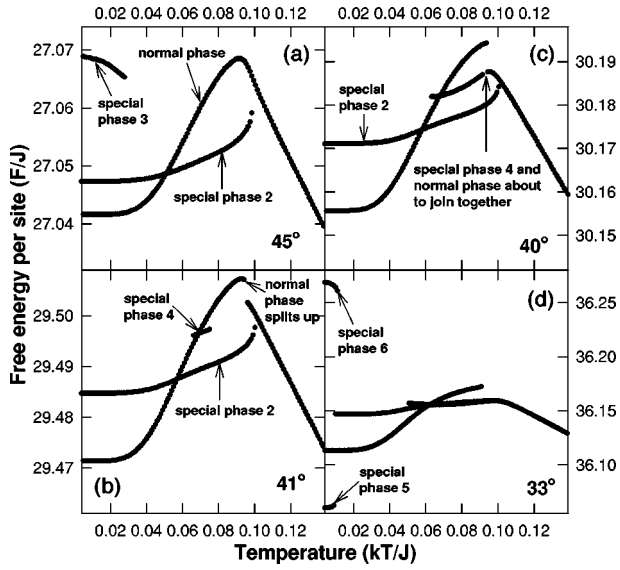


FIG. 9. The evolution of the free energy F vs temperature t from $\theta=45^\circ$ to $\theta=33^\circ$ with $n_{av}=2/3$.

<0.05 the normal state has lower free energy than special phase 2. There are two first-order transitions at about $t=0.10$ and at about $t=0.05$ for $\theta=45^\circ$. As the angle decreases down to $\theta=41^\circ$, special phase 3 disappears and a new phase of special phase 4 with average particle distribution $\{n_1, n_2, n_3, n_3, n_2, n_1\}$ appears at around $t=0.07$. Notice that the special phase 4 has the same type of average particle distribution as the normal phase, but with different values of n_i . Another change at this angle is that the free energy of the normal phase splits up into two curves with different phase properties at about $t=0.095$. At $\theta=40^\circ$, special phase 4 expands over a wider temperature range and gradually joins the normal phase at about $t=0.09$. At $\theta=33^\circ$, the two phases (special phase 4 and the normal phase) with similar average particle distribution finally join together, as shown in Fig. 9(d). On the other hand, two new phases, special phase 5 (with the lowest free energy) and special phase 6 (with the highest free energy) just emerge at very low temperature at this angle. The average particle distribution of special phase 5 is $\{n_1, n_2, n_3, n_4, n_5, n_6\}$ with ground state configuration $\{1, 1, 1, 1, 0, 0\}$, while the average particle distribution of special phase 6 is $\{n_1, n_2, n_3, n_3, n_2, n_1\}$ with ground state configuration $\{1, 1, 0, 0, 1, 1\}$. Notice that special phase 5 and special phase 6 have the same ground state configuration.

In Figs. 10(a)–10(d), we continue to illustrate the evolution of $F-t$ from $\theta=20^\circ$ to $\theta=0.5^\circ$. As the angle further decreases, both special phase 5 and special phase 6 spread out in temperature, as shown in Fig. 10(a). At $\theta=15^\circ$, special phase 6 joins the normal phase (note that these two phases have similar types of average particle distributions) at about $t=0.044$ and special phase 2 splits up at this temperature. At $\theta=5^\circ$, the normal phase and the special phase 5 overlap for $t<0.04$. For $0.04<t<0.10$, special phase 2, special phase 4, and the normal phase overlap. As the angle decreases down to 0.5° , the normal phase and special phase 6 both extend their range and combine into a single curve with average particle distribution $\{n_1, n_1, n_2, n_2, n_1, n_1\}$. It is

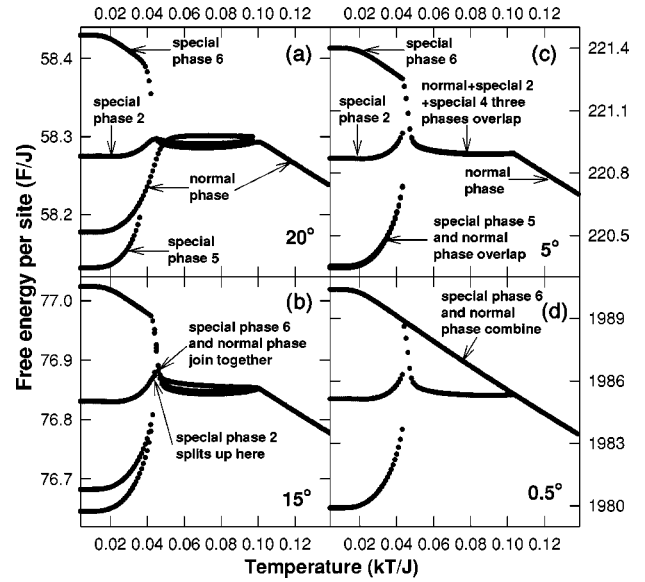


FIG. 10. The evolution of the free energy F vs temperature t from $\theta=20^\circ$ to $\theta=0.5^\circ$ with $n_{av}=2/3$.

noted that Fig. 10(d) is reminiscent of Fig. 4 of Ref. [1], except for the existence of special phase 2 for $t<0.04$. At these temperatures, as the angle approaches 0° , the lower two free-energy phases will overlap and the system will have the same properties as a straight chain. This result is reasonable, since the zigzag chain would behave like two well-separated and noninteracting straight chains as the angle approaches zero.

IV. DISCUSSION AND SUMMARY

In this paper, we utilize the LRMF method to study the partially occupied 1D zigzag chains with $1/r$ Coulomb interactions. We study the angular dependence of the phase properties in this 1D lattice gas system. Our calculations show that the system has complex thermodynamic properties and that the properties of the phase transitions are extremely sensitive to the occupancy n_{av} and zigzag angle θ . Generally, at large angles ($\theta>120^\circ$) zigzag chains exhibit properties similar to the straight chain system. At very small angles ($\theta<1^\circ$), zigzag chains can be viewed as two well-separated and noninteracting straight chains, and the system exhibits straight chain properties. For intermediate angles, the phase properties of these systems become rather complex and several possible solutions with different average particle distribution $\{\langle n_i \rangle\}$ are available at low temperatures for various n_{av} .

We found that the occupancy n_{av} of the partially occupied zigzag chain can be classified into two types. If n_{av} can be written as the simplest fractional form $n_{av}=r/p$, we define the occupancy to be “first type” if p is an even number and to be “second type” if p is an odd number. For example, $n_{av}=\frac{1}{2}$ or $\frac{3}{4}$ is first type and $n_{av}=\frac{2}{3}$ or $\frac{4}{5}$ is second type. The reason we make such a classification is that the calculated ground state configuration for a partially occupied zigzag

chain is different from a straight chain if p is even (first type), while the ground state for a zigzag chain and the straight chain is the same if p is odd (second type). According to our calculations, the phase properties alter drastically as the angle changes from 180° (straight chain) to approaching 0° in the partially occupied zigzag chain. For occupancy of first type, there is a critical angle θ_C at which the properties of the phase transitions change abruptly in the partially occupied 1D zigzag chain. For $n_{av} = 1/2$, there is an abrupt change of the phase properties at about $\theta_C = 86^\circ$ as the system transits from single chain mode (larger θ) to double chain mode (smaller θ) at this angle. On the other hand, there is no such distinct boundary for systems of the second type. For $n_{av} = 2/3$, the angular dependence of phase property in the partially occupied zigzag chain is much more complex than the case of $n_{av} = 1/2$. There are seven possible solutions in the $n_{av} = 2/3$ zigzag chain, existing in various angle intervals and temperature ranges.

Most interestingly, we found that the average particle distribution of the mixed phase is a linear combination of the special phase and the dual special phase for $n_{av} = 1/2$. The reason for the existence of the mixed phase is presumably due to the crossover of phase property from single chain mode (large angle) to double chain mode (small angle) in decreasing angle. According to our calculation a critical angle at about $\theta_C = 86^\circ$ separates these two modes, as mentioned above. In the vicinity of this particular angle, the tendency of being in the single chain mode or double chain mode is comparable, so that it is sensible that the system appears in a mixed phase with the phase property in the form of a linear combination of the single chain mode and double chain mode. At larger (smaller) angles the mixed phase shows more of the single (double) chain characteristics, as shown in the lower panel of Fig. 6 (Fig. 7).

Another intriguing feature is the reentrance of the normal phase in the phase property of partially occupied 1D zigzag chain. For example, for $n_{av} = 1/2$ ($\theta = 86.5^\circ$) the phase evolves from normal phase to mixed phase to normal phase to special phase in decreasing temperature (see upper panel of Fig. 6) and for $n_{av} = 2/3$ ($\theta = 120^\circ$) the phase evolves from normal phase to special phase to normal phase to special phase 2 in decreasing temperature (see upper panel of Fig. 8). This reentrance phenomenon is essentially a consequence of energy factor. In our model, a phase transition will occur

as long as a set of $\{n_i\}$ with a lower free energy appears at some temperature. In the $n_{av} = 1/2$ ($\theta = 86.5^\circ$) case, both solutions of the normal phase and the mixed phase are available for $0.012 < t < 0.03$. However the system will exhibit the mixed phase in this temperature range since the mixed phase has a lower free energy than the normal phase. At $t = 0.012$ the system must reenter the normal phase as the mixed phase disappears at this temperature. The same argument also holds for the $n_{av} = 2/3$ ($\theta = 120^\circ$) case, which in turn explains the reentrance of the normal phase in our model system.

We also calculate a real case: $\text{KCu}_{6.88}\text{S}_4$ with $n_{av} = 0.72$ ($\theta = 112.74^\circ$). Our calculated results show that the model system exhibits only one phase transition at $T_C = 0.044J/k$ (corresponding to 2400 K). However, the experiment results show that the Q1D material $\text{KCu}_{6.88}\text{S}_4$ exhibits two phase transitions at 205 K and 180 K [3]. Note that the zigzag chains in $\text{KCu}_{6.88}\text{S}_4$ have $(3 - 0.12)$ out of 4 equivalent sites for Cu atoms on the chain occupied, so that $n_{av} = 0.72$. The possible reasons for these inconsistencies between our calculations and experimental results could be among the following.

(1) The interchain interactions between the zigzag chains, which were not considered in our model, should play important roles in the phase properties of this system.

(2) The shielding effect of the Coulomb interaction between neighboring particles should be taken into account in the model to obtain consistent transition temperature between theory and experiment. In the present case, a Coulomb shielding parameter of 3.5 would yield a reasonable transition temperature for the $\text{KCu}_{7-x}\text{S}_4$ system.

(3) The mean-field approximation we employed in this model. Finally, it is obvious that the establishment of a three-dimensional model is necessary to further understand the mechanism of the phase transitions exhibited in the $\text{KCu}_{7-x}\text{S}_4$ system.

ACKNOWLEDGMENTS

This work was supported by National Science Council, Taiwan, Republic of China, under Grant No. NSC-90-2112-M-213-003 (T.C.K) and Grant No. NSC-91-2112-M-259-015 (Y.K.K). The calculations were performed on the high speed computers at the National Center for High-Performance Computing, Taiwan.

-
- [1] T.C. King, Y.K. Kuo, M.J. Skove and S.-J. Hwu, Phys. Rev. B **63**, 045405 (2001).
 [2] T.C. King, Y.K. Kuo and M.J. Skove, Physica A **313**, 427 (2002).
 [3] Y.-K. Kuo, M.J. Skove, D.T. Verebelyi, H. Li, R. Mackay, S.-J. Hwu, M.-H. Whangbo, and J.W. Brill, Phys. Rev. B **57**, 3315 (1998).

- [4] S.-J. Hwu, H. Li, R. Mackay, Y.-K. Kuo, M.J. Skove, M. Mahapatro, C.K. Bucher, J.P. Halladay, and M.W. Hayes, Chem. Mater. **10**, 6 (1998).
 [5] H. Li, R. Mackay, S.-J. Hwu, Y.-K. Kuo, M.J. Skove, Y. Yokota, and T. Ohtani, Chem. Mater. **10**, 3172 (1998).
 [6] M. Brack, Rev. Mod. Phys. **65**, 677 (1993).